A Dictionary-Based Bayesian Approach to Optimizing Left-Turn Restriction Locations in Grid Networks

Dongqin Zhou*

The Institute for Experiential AI
Northeastern University, Boston, MA
Email: d.zhou@northeastern.edu

Vikash V. Gayah

Department of Civil and Environmental Engineering The Pennsylvania State University, University Park, PA Email: gayah@engr.psu.edu

* Corresponding author.

ABSTRACT

Left-turn movements at signalized intersections pose significant safety risks for the drivers and efficiency concerns for the traffic operations in urban networks. Restricting left-turn movements at selected locations has been shown to be effective at improving operational efficiency and mitigating safety concerns. However, determining optimal locations to restrict left-turns is a complex combinatorial optimization problem that is compounded by the lack of analytical forms for the objective function and constraints, as well as potential interdependencies between the decision variables. Following the common solution paradigm for this type of optimization problems, this paper presents a novel Bayesian approach that utilizes dictionary-based embeddings and is tailored for high-dimensional combinatorial (or even mixed) spaces. Simulation studies conducted using the Aimsun software under perfect or imperfect grid networks demonstrate that the presented method can consistently find promising left-turn restriction configurations that outperform the all-or-nothing strategies (to restrict all or none left-turn movements at all intersections), as well as the population based incremental learning algorithm. In addition, the presented method often does so with less simulation cost, thus showcasing its potential for efficient solution of more general traffic optimization problems.

Keywords: Left-turn restriction; Bayesian approach; Black-box combinatorial optimization

1. Introduction

Ensuring efficient traffic operations in urban areas has long been a priority for transportation researchers and practitioners. Arguably, signalized intersections play the most important role in managing traffic for urban road networks. How to simultaneously ensure safety and efficiency at signalized intersections has been driving the designs of signal phasing and timing plans (Cottrell Jr, 1986; Roess et al., 2010) as well as the recent (yet extensive) development of traffic signal control strategies using advanced technologies (Chen et al., 2020; Chu et al., 2020; Wei et al., 2019, 2018).

At signalized intersections, extra care must be paid to left-turn movements since these turning vehicles need to cross the paths of opposing through-moving vehicles to traverse the intersection. The left-turn maneuvers thus present significant risks for the safety of the drivers and operational efficiency of the intersections (or even the whole network should some intersections break down due to crashes). Serving the left-turn vehicles in protected phases can help eliminate the potential risks to the drivers by completely segregating the times in which opposing through vehicles and left-turn vehicles move. However, protected phases induce additional lost times (thus decreasing the total time the intersection is serving vehicles) and take time away from throughmoving vehicles (thus further reducing the time the intersection is serving through movements which tend to have the highest discharging rate) (Messer and Fambro, 1977; Newell, 1959). Furthermore, protected left-turn phases often require the installation of dedicated left-turn lanes, which may be overly expensive for dense urban areas. Permitted left-turn movements yield more efficient but considerably less safe operations at the intersections since the left-turn vehicles are moving while the through-moving vehicles are also in motion. Sufficient gaps must exist for the turning vehicles to move, and long queues could form in the presence of heavy traffic, even with dedicated left-turn pockets (Haddad and Geroliminis, 2013). Compound phases serve the left-turns in a protected-permitted fashion but still are faced with safety as well as efficiency concerns.

To jointly realize safety and efficiency objectives at signalized intersections, alternative network or intersection designs have been developed and evaluated in the past. For example, unidirectional street networks have the potential to alleviate left-turn conflicts and provide higher traffic flows and travel speeds (Stemley, 1998). However, these benefits can often be offset by the resulting negative externalities such as safety concerns due to the increased travel speeds and more tendency of the drivers to run red lights, as well as reduced economic activity (Walker et al., 2000; Wazana et al., 2000). Numerous atypical intersection designs have also been proposed as viable ways to accommodate conflicting left turns (Berkowitz et al., 1996; Chowdhury, 2011; Joseph and John, 2000; Reid and Hummer, 2001; Xuan et al., 2011), yet these designs often require large spatial footprints or additional infrastructure than conventional intersections due to their complex geometries, which thus render them not applicable in dense urban areas.

One comparatively simpler approach is to restrict the left-turns at signalized intersections. In this way, the conflicts between left-turn and opposing through-moving vehicles are reduced, limiting the most dangerous type of crashes at intersections (Chan, 2006). Further, doing so improves the operational efficiency at the intersections as a result of fewer lost times and the use of more lanes exclusively for through/right-turn movements with higher discharging rates. Note, restricting left turns at intersections improves both safety measures (by reducing traffic conflicts) and operational efficiency, but in this work the analytical focus is more on the latter with safety measures left as a future research extension. The main drawback of restricting left turns is that

vehicles that would otherwise turn left now need to travel longer distances, increasing the average travel distances for all vehicles. To gain a holistic view of this left-turn restriction strategy at the network level, several studies have adopted macroscopic traffic flow models to examine its operational performances (DePrator et al., 2017; Gayah and Daganzo, 2012; Ortigosa et al., 2019, 2017). The findings suggest that network-wide restriction of left-turn movements at all intersections could increase the trip completion rate (i.e., rate that vehicles arrive at their destinations), especially when the network is operating around its capacity. These studies indicated the prospects of left-turn restriction for grid networks, yet they focused on network-wide treatment and did not consider a partial restriction profile that is more flexible and suitable for different demand or congestion situations.

Unfortunately, determining the optimal locations to enact left-turn restriction in a grid network is challenging, and the reasons are multifold. First, the problem does not admit explicit forms for the objective function or constraining conditions. As such, mathematical optimization techniques (such as nonlinear or integer optimization) are not applicable. Existing studies that adopted analytical methods to left-turn restriction have instead relied on simplistic traffic models that failed to capture queue dynamics or vehicle routing (Tang and Friedrich, 2018, 2016). Second, the problem has a combinatorically large solution space for which even a partial enumeration can be intractable. Furthermore, the large solution space is compounded by potential interdependences between the decision variables (i.e., intersections to enact the left-turn restriction); that is, left-turn restriction applied at one intersection will affect operations (e.g., vehicle arrival and routing) at the adjacent intersections which thus influence the left-turn restriction policy at those intersections. Despite the challenges, however, there have been some recent breakthroughs in determining the optimal left-turn restriction locations for grid networks. In (Bayrak et al., 2023), a populationbased incremental learning (PBIL) algorithm was utilized to determine promising left-turn restriction configurations, but the interdependencies between decision variables are not accounted for. To address the unaccounted dependencies, a Bayesian optimization algorithm (Pelikan et al., n.d.) was adopted in (Bayrak and Gayah, 2021), where a hybrid method integrating the exploration capability of PBIL was also presented. Both works have used microsimulation as a replacement for the simple traffic models to ameliorate the lack of analytical forms for the objective function and constraints as well as the need of realistic responsive traffic (e.g., dynamic vehicle routing) when evaluating the left-turn restriction configurations.

Along the lines of these recent works, this paper presents a novel Bayesian approach to determining optimal left-turn restriction locations for grid networks. Using dictionary-based embeddings, the presented approach converts the black-box combinatorial optimization problem into one that is defined on continuous spaces for which canonical black-box solution methods are applicable. More importantly, the approach could reduce the cardinality of the search space which serves to accelerate the solution process. In contrast, the Bayesian optimization algorithm adopted in (Pelikan et al., n.d.) do not possess these desirable properties. Further, the Bayesian algorithms in (Pelikan et al., n.d.) utilize a random sampling process to generate the next iteration of solutions, which, comparatively, are generated by an optimization procedure using the presented approach herein. Such a procedure indicates higher potential of yielding more performant solutions in the iterative process. To showcase the effectiveness of the presented approach, the PBIL algorithm (Baluja, 1994; Bayrak et al., 2023) is applied for comparison and the restriction configurations are evaluated using the Aimsun microsimulation platform.

The rest of the paper is outlined as follows. The next section explains the proposed methodology where the PBIL algorithm is also discussed. The simulation setups are then presented, followed by the simulation results. Concluding remarks are provided in the final section.

2. METHODOLOGY

The first subsection of this section provides an overview of the population-based incremental learning algorithm. The next subsection reviews the literature on Bayesian optimization and the adopted approach is described in the last subsection.

2.1 Population-Based Incremental Learning (PBIL)

PBIL is heuristic method that combines features of genetic algorithms with competitive learning (Baluja, 1994). It adopts an incremental structure where the solutions visited so far will be utilized to inform the next (set of) solutions. Such incremental structure along with the heuristic search nature makes the PBIL method suitable for high-dimensional black-box optimization problems as considered in this work, and it has been shown capable of determining promising left-turn restriction profiles in urban grid networks (Bayrak et al., 2023; Bayrak and Gayah, 2021). Specifically, the PBIL method executes a sequence of four steps iteratively until termination: initialization, generation, evaluation, and update. First, a probability vector is initialized, as used to generate a group of candidate solutions that are evaluated using the Aimsun software. The evaluation results then inform updates of the probability vector which further helps generate an improved group of solutions. In the following, these steps are explained in greater detail.

The initialization step creates an initial probability vector P^1 whose number of elements is the same as the number of candidate intersections that are considered for left-turn restriction implementation. Each element indicates the likelihood or probability of left-turn restriction being enacted at the intersection. Thus, at the initialization phase, all elements are set to a value of 0.5 to represent completely random decisions; that is, at the first iteration, the decision of whether to restrict left-turn movements is made at random for each intersection and does not build upon any prior knowledge about the traffic demand or network structure.

The generation step generates a population of N possible left-turn restriction configurations based on the probability vector P^t at iteration t, where N denotes the population size. Note that the restriction configurations are represented using a binary vector where restricting the left turns is indicated by 1 and 0 otherwise. The evaluation step at iteration t then assesses the quality of the population of the left-turn restriction configurations using microsimulation. The total travel time mentioned above is used as a metric to rank the configurations, and the best and worst configurations at this iteration are denoted by b^t and w^t .

After evaluation, the best and worst configurations are used to update the probability vector to improve the quality of the next generation of population. Updating the probability vector involves positively learning features from the best configuration and negatively learning (avoiding) features from the worst configuration, as well as random mutations. Specifically, positive learning leads the algorithm to favor left-turn restriction decisions of the best configuration by updating the probability vector towards it:

$$P_i^{t+1} = P_i^t \times (1 - LR^+) + b_i^t \times LR^+ \tag{1}$$

where LR^+ denotes the positive learning rate and b_i^t is the *i*-th left-turn restriction decision at iteration t (for the *i*-th intersection) in the best configuration. Intuitively, Eq. (1) means to decrease the probability of restricting the left-turn movements at intersection i if they are not restricted in the best configuration (i.e., $b_i^t = 0$). On the contrary, left-turn restrictions should be more likely to be enacted at intersection i if they appear in the best configuration (i.e., $b_i^t = 1$). In a similar fashion, negative learning leads the probability vector away from the worst configuration:

169
$$P_i^{t+1} = P_i^t \times (1 + LR^-) - w_i^t \times LR^-$$
 (2)

where LR^- denotes the negative learning rate and w_i^t is the *i*-th left-turn restriction decision at iteration t (for the *i*-th intersection) in the worst configuration.

The positive and negative learning rates jointly control the speed of convergence. To further expand the amount of exploration performed to the solution space and thus improve the quality of the converged solution, each element of the probability vector is randomly mutated by a magnitude Δm with probability m according to:

$$P_i^{t+1} = P_i^t \times (1 - \Delta m) + \Delta m \tag{3}$$

With the combination of learning updates and mutation, the PBIL algorithm adequately explores the solution space and learns useful features from past solutions to improve future generated solutions. The iterative process continues until some stopping criteria are reached. In this paper, the PBIL algorithm terminates after 20 iterations. The population size is set to N = 50, so a total of 1000 configurations will be evaluated. This evaluation budget makes the run time of each experiment manageable. The population size of 50 ensures a diverse enough group of candidates per generation while in the meantime ensures there will be enough generations to produce a promising solution. The learning rates and mutation parameters are $LR^+ = 0.1$, $LR^- = 0.075$, $\Delta m = 0.05$, m = 0.02. These values are selected to be consistent with (Bayrak et al., 2023).

2.2 Bayesian Optimization

The problem of determining optimal locations for left-turn restrictions in a grid network is complicated due to the lack of analytical form for the objective function and constraints, which are compounded by the large solution space and potential interactions between the decision variables. For this problem, one only has access to the inputs (i.e., the candidate left-turn restriction configurations) and outputs (i.e., the total travel time, TTT) of the system and cannot afford to evaluate every possible input. As such, this problem naturally falls into the realm of black-box optimization, which arises ubiquitously in engineering problems. The most common example is hyperparameter tuning (Snoek et al., 2012), which involves selecting the best hyperparameter configuration that minimizes a certain loss (e.g., validation loss).

For these black-box optimization problems, Bayesian optimization (BO) has attracted intensive research interests due to its expressiveness and efficiency, and it has been shown significantly superior to random search (Turner et al., 2021). Specifically, BO methods utilize particularly expressive probabilistic surrogate models to approximate the costly-to-evaluate black-box objective functions. An acquisition function associated with the surrogate model is then optimized to yield the next evaluation point. The next evaluation point together with its function value is then used to update the surrogate model, which is in turn used to produce the subsequent evaluation points. This iterative process is executed until termination, for example until the number

of function evaluations reaches a certain limit. Compared to the PBIL algorithm which only uses the best and worst configurations to update the probability vector, BO methods are significantly more sample efficient since all configurations evaluated are used to update the surrogate model.

The most common surrogate model used in BO methods is Gaussian processes (GP) (Rasmussen and Williams, 2006), which directly define a probabilistic distribution for the black-box objective function. Let x denote an evaluation point, which in this work represents a left-turn restriction configuration. Denote as f(x) the black-box objective function which represents the TTT associated with the restriction configuration x. A Gaussian process assumes any finite number of the function values are jointly normally distributed:

$$p(f|X) = \mathcal{N}(f|\mu, K) \tag{4}$$

where $f = (f(x_1), \dots, f(x_n))$ and $X = (x_1, \dots, x_n)$ are respectively vectors of function values (TTT) and restriction configurations, p is the GP prior, \mathcal{N} is a multivariate normal distribution, μ is the mean of the GP prior that is commonly set to $\mathbf{0}$, and K is a matrix of covariance functions. Given a list of left-turn restriction profiles X and the TTT values f, the GP prior can be converted into a GP posterior that can then be used to predict the function value for any new left-turn restriction profile, say x^* . The GP predictions will be in the form of a Gaussian distribution with a mean value (denote as $\mu(x^*)$) and a standard deviation (denote as $\sigma(x^*)$); in other words, the predictions are probabilistic rather than deterministic. In this way, the GP posterior provides an approximate model for the black-box objective function, where the function value at any input x^* is quantified by a mean of $\mu(x^*)$ and a standard deviation of $\sigma(x^*)$.

Deciding the next left-turn restriction configuration to evaluate involves balancing the amount of exploration (i.e., to choose a configuration with high uncertainty) and exploitation (i.e., to choose one with high predicted objective function), and acquisition functions are utilized in Bayesian optimization methods for this task. The most popular choice of acquisition function is expected improvement, which quantifies the expected benefits of choosing a certain configuration over the incumbent best in terms of the function value. This metric takes into account both the mean predictions from the surrogate model and the related uncertainty. Formally, the expected improvement of a point x^* is defined as

$$\alpha_{EI}(x^*) = \mathbb{E}[\max(f(x^*) - f(x^+), 0)] \tag{5}$$

where $\alpha_{EI}(\cdot)$ denotes the acquisition function with expected improvement, x^+ is the current best solution, and $f(x^+)$ is the current best function value. In Eq. (5) improvement means larger function values, whereas the objective of left-turn restriction is to minimize TTT. Thus, during implementation, the function value returned is changed to the negative TTT. Since the surrogate model is a Gaussian process, the acquisition function enjoys an explicit analytical form (Jones et al., 1998):

$$\alpha_{EI}(x^*) = \left(\mu(x^*) - f(x^*)\right) \Phi\left(\frac{\mu(x^*) - f(x^*)}{\sigma(x^*)}\right) + \sigma(x^*) \phi\left(\frac{\mu(x^*) - f(x^*)}{\sigma(x^*)}\right) \tag{6}$$

where $\Phi(\cdot)$ and $\phi(\cdot)$ are respectively the cumulative distribution function and probability distribution functions of the standard normal distribution. Intuitively, the first part of Eq. (6) encourages exploitation (higher mean predicted objective function value $\mu(x^*)$) while the second part encourages exploration (higher uncertainty associated with the prediction $\sigma(x^*)$). Maximizing

the acquisition function thus considers both and yields the most promising point for the next evaluation.

Despite its expressiveness and efficiency, however, BO methods have been historically limited to problems with modest dimensionality and exclusively continuous search spaces. Only recently have researchers extended Bayesian optimization to high-dimensional, combinatorial, or even mixed spaces (i.e, a mixture of both combinatorial and continuous decision variables). Highdimensional continuous spaces were considered in (Eriksson et al., 2019; Eriksson and Jankowiak, 2021; Papenmeier et al., 2023), among which (Eriksson et al., 2019) realizes the strongest baseline performance in the Black-Box Optimization Challenge (Turner et al., 2021). Pioneering works in the combinatorial space include (Baptista and Poloczek, 2018; Oh et al., 2019), yet the cost of learning the surrogate model and drawing the next evaluation point is even higher than actually evaluating it using the black-box function. This thus limits their applicability to high-dimensional problems. There are also non-Bayesian approaches to black-box combinatorial problems like (Dadkhahi et al., 2022, 2020), but they are generally less sample efficient than the Bayesian counterparts. BO methods for mixed spaces are comparatively less explored. In (Ru et al., 2019), a hybrid strategy was adopted to optimize over categorical and continuous domains which involves a multi-armed bandit and a conventional GP-based BO method, yet the strategy is not applicable in high-dimensional spaces. Recent efforts like (Daulton et al., 2022; Deshwal et al., 2023; Wan et al., 2021) have proposed methods that are sample efficient in high-dimensional mixed spaces, and they have utilized techniques like Hamming embeddings or probabilistic reparameterization.

2.3 Bayesian Optimization with Dictionary-Based Embeddings

245

246

247

248

249

250

251

252

253

254

255

256

257

258

259

260

261

262263

264

265

266267

268

269

270

271

272

With the ability to address the large solution space as well as interdependencies between decision variables, BO methods are utilized herein to determine the optimal left-turn restriction profiles in grid networks. Further, a design to explicitly deal with the combinatorial structure of the problem is particularly helpful. For this reason, the dictionary-based approach proposed in (Deshwal et al., 2023) (referred to as BODi) is adopted, which is formally shown in Algorithm 1. In the following, the building components of the method are explained.

```
274
        Algorithm 1. A Dictionary-Based Bayesian Approach to Optimizing Left-Turn Restriction
        Locations
275
276
        1: Inputs: dimensionality of search space d, dictionary size k, number of function evaluations T,
277
                   initial training data size l, empty dataset D
278
279
        2: for iter = 1 to T do
280
                 // generate random training samples of size l
        3:
281
        4:
                 if iter \leq l then
                          \mathbf{z}_{iter} = a random restriction configuration drawn from the search space \{0, 1\}^d
282
        5:
283
                          Evaluate the sample using microsimulation and obtain the total travel time (TTT)
        6:
284
                         f(\mathbf{z}_{iter}) = (-1) \times TTT; D = D \cup \{\mathbf{z}_{iter}, f(\mathbf{z}_{iter})\}
        7:
285
                         continue
        8:
286
        9:
                 end if
287
                 // construct dictionary of size k \times d
        10:
288
                 Initialize empty dictionary A
        11:
289
        12:
                 for i = 1 to k do
290
        13:
                          a_i \leftarrow \text{empty}
291
        14:
                          Sample Bernoulli parameter \theta \sim \text{Uniform } (0,1)
292
        15:
                          for j = 1 to d do
293
        16:
                                  Sample binary number a \sim \text{Bernoulli}(\theta)
294
        17:
                                  a_i \leftarrow a_i \cup a
295
        18:
                          end for
296
        19:
                          Add a_i to dictionary: A \leftarrow A \cup a_i
297
        20:
                 end for
298
        21:
                 // compute Hamming embedding space using dictionary A
299
        22:
                 Initialize an empty set of Hamming embeddings M
300
        23:
                 for each restriction configuration z \in D do
301
        24:
                          Initialize empty embedding e_z
302
        25:
                          for i = 1 to k do
303
        26:
                                  [e_z]_i = h(a_i, z) // compute Hamming distance
304
        27:
                          end for
305
                          M \leftarrow M \cup e_z
        28:
306
        29:
                 end for
307
        30:
                 // canonical Bayesian Optimization steps
308
                 Fit a Gaussian Process \mathcal{GP}_{M} using the embeddings M and function values f
        31:
                 Maximize the acquisition function using local search to obtain the next evaluation point
309
        32:
                 \mathbf{z}^* = \arg\max_{\mathbf{z}} \alpha_{EI}(\mathcal{GP}_{\mathbf{M}})
310
311
                 Evaluate the point z^* using microsimulation and obtain the total travel time (TTT^*)
        33:
312
                 f(\mathbf{z}^*) = (-1) \times TTT^* D = D \cup \{\mathbf{z}^*, f(\mathbf{z}^*)\}\
        34:
313
314
        35: end for
        36: return \mathbf{z}_{best} = \arg \min\{f(\mathbf{z}_1), f(\mathbf{z}_2), \dots\}, f_{min} = \min\{f(\mathbf{z}_1), f(\mathbf{z}_2), \dots\}
315
316
```

The core design idea behind BODi is the use of a dictionary, which is a fixed number of candidate structures (i.e., candidate left-turn restriction profiles) from the input space. The dictionary is constructed at each iteration using the randomized procedure as detailed in lines 10-20 of Algorithm 1. By computing the Hamming distance (i.e., the number of bits that are different at the same position in two sequences, denoted as h(,) in Algorithm 1) between an input (say, z) and elements of the dictionary, one obtains the Hamming embedding e_z , which is a continuous vector of the same size as the dictionary (k). Thus, the Hamming embeddings convert the original problem defined in a combinatorial space into one defined in a continuous space, and Gaussian processes can be used as surrogate models. Importantly, dictionary-based embeddings can facilitate a cardinality reduction of the embedded search space, which helps accelerate optimization and ensure fast convergence. The theoretical analyses of the dictionary construction as well as the regret bound for the BODi method can be found in (Deshwal et al., 2023).

Utilizing the Hamming embeddings and the function values \boldsymbol{f} , a Gaussian process surrogate model can be fitted. The expected improvement acquisition function is then maximized using local search to produce the next evaluation point. Specifically, a group of random initial restriction configurations are generated, from which the top-ranked candidates are picked and used as starting points for local search. The local search moves to one-Hamming distance neighbors of each starting point to find a candidate with the highest acquisition function value. From the selected candidates the local search is repeated for another step. In this work, a total of 20 local search steps are executed, and the next evaluation point is the best candidate among all local search trajectories. The next evaluation point is then simulated using Aimsun and added to the dataset along with the associated function value (negative TTT). The dictionary construction procedure and subsequent steps are then repeated in the following iteration.

In the present work, the initial training dataset size is set to l=50, the dictionary size is k=128, and the total number of function evaluations is T=1000 which is the same as the number of configurations evaluated by PBIL. The dimensionality of the search space depends on the left-turn restriction decisions made for each intersection. For example, when a single restriction decision is made for all approaches at an intersection, the dimensionality is set to d=60, i.e., a total of 64 intersections minus four corner ones where left-turn restriction is never applied. Further, note that the parameter values are decided mainly in reference to the values utilized in (Deshwal et al., 2023) instead of an intricate tuning process. While tailored parameter values might be helpful, the experiment results suggest that the presented BODi method is sufficiently performant compared to PBIL using these values, which shows it is not sensitive to the parameter choices.

3. SIMULATION SETUP

The effectiveness of different approaches to determining optimal left-turn restriction locations can be compared by evaluating the derived restriction configurations. To facilitate accurate evaluations and thus fair comparisons, the Aimsun microsimulation platform is used for its ability to realistically simulate traffic responses to the left-turn restrictions (e.g., dynamic vehicle routing) as well as various traffic phenomena such as queue spillbacks and congestion propagation.

The first network considered has a perfect grid structure of size 8×8 ; see Fig. 1(a). This structure is studied as grids (or grid-like structures) often appear in real-world street networks and could thus provide general insights about the management of left turns. Two-way traffic is assumed,

and every street has two lanes for each travel direction with a common block length of 250m. The capacity of each lane is set to 1600 veh/hr and the speed limit is 48 km/h. All intersections in the network are signalized and adopt a common fixed-time two-phase signal plan. The shared cycle length is 90s with 42s green time and 3s change interval for each phase. No offset is assumed as it is shown inconsequential to the network-level performances in grid networks (Girault et al., 2016). The simulation step is set to 1s. These settings mimic realistic urban networks and are consistent with prior works (Bayrak et al., 2023; Bayrak and Gayah, 2021).

In this network, the left-turn movements have two possible treatments at each intersection: allowed in a permitted fashion or restricted (with two types of restriction to be explained shortly). In the former case, the left-turn vehicles share the same lane with through-moving vehicles (likewise, the right-turn vehicles share lane with through-moving vehicles). As such, the left-turn movements, when permitted, do not require extra infrastructure, and when restricted, do not leave any existing infrastructure unutilized. Note, left-turn movements are never restricted at the four corner intersections to ensure at least one feasible and realistic path exists for each OD pair.

Without changing network parameters (e.g., link capacity, speed limit, etc.), an imperfect grid structure is also considered to compare the methods in a setting more representative of real-world situations; see Fig. 1(b). To construct this network, twelve half-block links are randomly removed from the perfect grid while keeping the connectivity between all OD pairs. Note, the links are removed directly from the network (rather than being temporarily misfunctioning from vehicle blockage), and as a result, previous routes that utilize these links are no longer feasible and the vehicles are routed using alternative paths at the beginning of simulation.

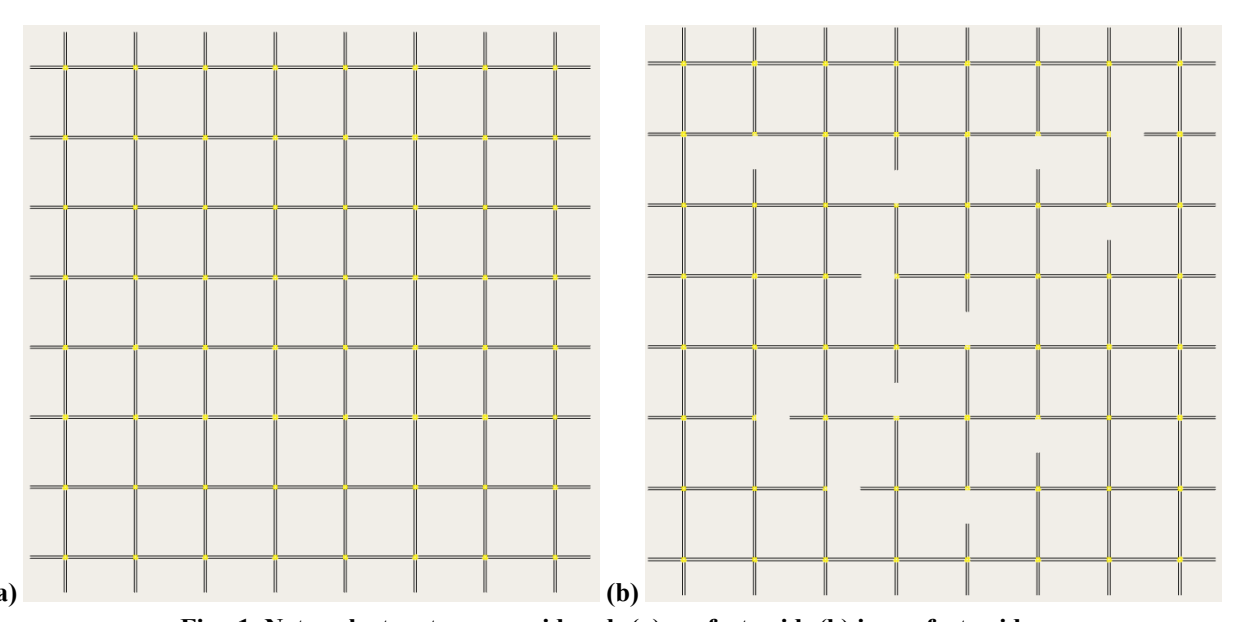


Fig. 1. Network structures considered: (a) perfect grid; (b) imperfect grid.

Origin and destination locations are evenly distributed across the entire network and placed at the 32 peripherical entry/exit points of the network as well as the mid-block points of each street. For illustration purposes, a uniform demand pattern is assumed where each origin (destination) generates (attracts) the same expected number of trips. However, the presented approaches are generic and applicable to any demand patterns. The cumulative number of vehicles generated from

the traffic demands is shown in Fig. 2, where the demand generation lasts for 45 minutes followed by a recovery period of 15 minutes to mimic the full dissipation of congestion. During demand generation, an average of 367 new vehicles are simulated each minute. Under such demand, the network is saturated when all left-turns are permitted, which serves to benchmark the other methods by comparing the traffic conditions with different restriction configurations. Importantly, note that while the traffic demand in Fig. 2 appears to be constant, the realized traffic demand will exhibit variability during each simulation instance (for example, the exact times when vehicles are inserted into the network will be changeable), and multiple random seeds will be used to enhance realism for the demand generation. Further, note that the cumulative count curve shown in Fig. 2 is also used in combination with the cumulative count curve of vehicle exits to calculate the total travel time (TTT) during the whole simulation. The TTT is used as the primary evaluation metric for the left-turn restriction profiles and thus a comparison metric for the different approaches.

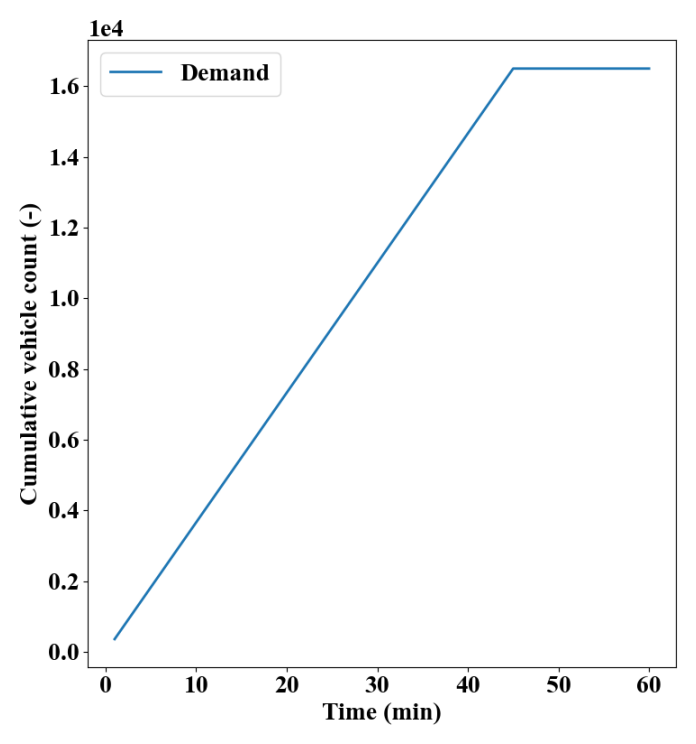


Fig. 2. Cumulative count curve of vehicle generation from traffic demands.

The simulated vehicles are initially routed using the stochastic C-logit route choice model (Cascetta et al., 1996), which mimics the stochastic user-equilibrium pattern. However, a subset of the vehicles (50%) were assumed to be able to reroute themselves based on the prevailing traffic (e.g., congestion conditions, perceived travel times, and changes of route availabilities from left-turn restriction) so as to minimize their own perceived travel cost, which resembles realistic driving behaviors. This adaptive rerouting has been shown helpful to the network-wide operational performances (Daganzo et al., 2011; Gayah and Daganzo, 2011), and in this work it happens at regular intervals of 3 minutes, similar to (Bayrak et al., 2023; Bayrak and Gayah, 2021). Note, such adaptive rerouting is always assumed in microsimulation, regardless of which method is used to determine the left-turn restriction profiles. A fair comparison among different left-turn restriction methods can thus be conducted.

4. RESULTS

This section presents the results of left-turn restriction configurations using PBIL and the proposed BODi method. For benchmarking purposes, two baseline configurations are also considered: permitted left-turns (PLT) everywhere and restricted left-turns (RLT) everywhere. These two baselines simulate all-or-nothing strategies where a single decision is made across the entire network. Comparisons with these demonstrate the need for intersection-level treatments of left-turn movements. Two optimization scenarios are considered for the perfect grid network: a) a single restriction decision is made for all approaches of an intersection; b) a restriction decision is made for each competing direction (i.e., NS and EW) of an intersection. Excluding the four corner intersections where left-turn restrictions are not considered to maintain paths for vehicles entering/exiting at these locations, the former (latter) scenario has a search space of dimensionality 60 (120). This means 2⁶⁰ (2¹²⁰) combinations that must be considered to test the entire solution space, which makes enumeration methods inapplicable. Thus, the global optimal configuration is not available and the optimality gap unknown.

4.1 Perfect Grid Network

Traffic simulations generally involve random processes that impact the trip generation and OD pattern (and subsequently the routing decisions), and such randomness is often specified by the random seed used. In light of this, multiple random seeds are considered for the perfect grid network which simulate day-to-day variations of the traffic patterns. Each seed corresponds to a simulation instance with a specific traffic pattern (e.g., trip generation). This helps examine the consistency and robustness of the methods. Moreover, both methods (PBIL and BODi) involve a sizable amount of randomness in the inherent solution processes, hence they conduct three optimization runs for each simulation instance and the best-found configuration is reported for each instance.

The first scenario (a single decision per intersection) is considered. The minimum total travel times (TTT) achieved by PBIL and the proposed method (among three optimization runs) for the 6 simulation instances are presented in Fig. 3, together with the two baseline configurations. As can be observed, the all-or-nothing strategies (restricting the left-turn movements everywhere or nowhere) generally do not perform as well as the methods where left-turn movements are only restricted partially at selected intersections. Noticeably, restricting left turns at all intersections is considerably worse than permitting them, which is likely due to the significant number of detours incurred by the restrictions. While in high-demand situations such restrictions can be beneficial (DePrator et al., 2017; Gayah and Daganzo, 2012), in modest demand scenarios such as the one considered here a partial restriction or even no restriction is much preferred. More importantly, Fig. 3 suggests that the proposed method consistently outperforms PBIL with lower realized TTTs, with varied differences across simulation instances. This showcases the effectiveness of the BODi method for determining promising left-turn restriction locations.

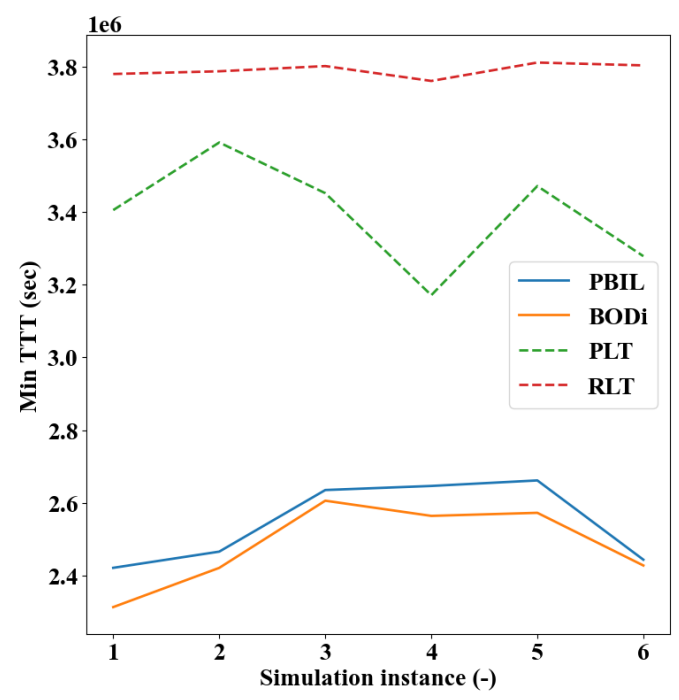


Fig. 3. Min TTT achieved by different methods under various simulation instances.

458 459

460

461

462

463

464 465

466

467

468

469

470

471

472

473

474

475

476

Both the PBIL and proposed BODi method adopt a solution procedure where the probability vector or surrogate model is updated iteratively, and these updates can be loosely viewed as a learning process. To compare their abilities to learn from past experiences, the TTTs of the incumbent best solutions throughout the learning processes are visualized in Fig. 4. Note that, in each PBIL iteration a group of 50 configurations are evaluated whereas only one is evaluated by the BODi method per iteration. To facilitate the comparison, every 50 configurations evaluated by BODi are grouped together and treated as a "mega" iteration. Also, Fig. 4 provides the fraction of time (next to the subplot titles) when BODi outperforms PBIL during the learning processes. Further, notice that the TTTs of the baseline configurations (PLT and RLT) are constant for each simulation instance, which is expected as the baseline configurations are not iteratively updated. As Fig. 4 reveals, both methods can effectively learn from the past configurations and their related function values and use these experiences to improve the quality of subsequently selected solutions. Importantly, the BODi method can often realize noticeably smaller min TTTs than PBIL (instance 1, 4, 5), and for almost all instances (except instance 2) BODi outperforms PBIL most of the time during the learning processes. Further, notice that while PBIL seems to converge faster, it fails to produce as competitive solutions as BODi does. This suggests the PBIL is potentially trapped in a local solution due to its limited exploration capability compared to BODi.

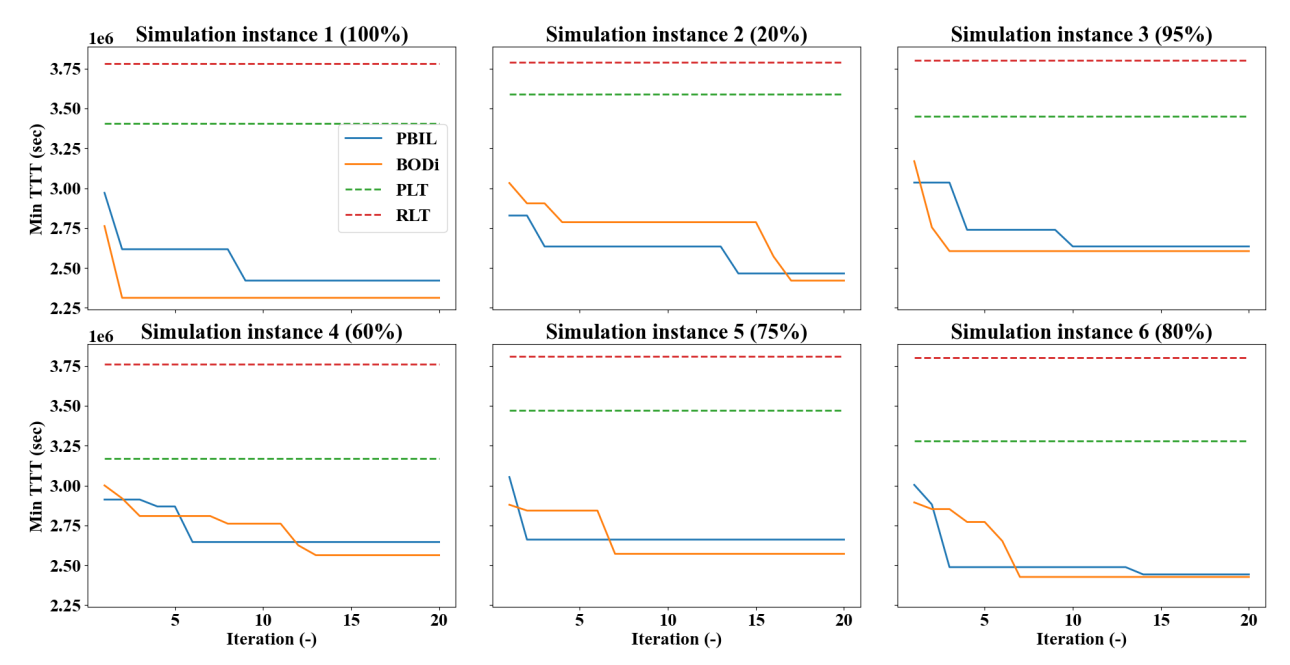


Fig. 4. Min TTT achieved over time by different methods under each simulation instance.

478

479 480

481

482

483

484

485

486 487

488

489

490

491

492

493

494

495

496

497

498

The variability of solutions visited by both the PBIL and BODi methods are further examined to compare their learning processes. To this end, note the solution (i.e., a left-turn restriction configuration) is represented by a binary vector of dimension 64, which can thus be uniquely identified by the distance to the origin in a space of dimension 64. Hence, the variability of solutions can be reflected by the summary statistics of the distance measurements of these solutions. Fig. 5 shows the summary statistics of solutions found by both methods during the entire learning process, under each simulation instance and in the form of box plots. The subplots also provide the ratios of interquartile range of BODi over PBIL (denoted as IOR Ratio). As can be seen, in all simulation instances, the BODi method has a wider interquartile range than PBIL. This wider interquartile range of the BODi method is also often associated with better solutions over PBIL; for example see simulation instances 1, 4, 5 in Fig. 4 and Fig. 5. As an illustration, the variability of solutions across learning iterations under simulation instance 1 is also presented in Fig. 6. The median values of the iteration-wise box plots are connected, whose coefficients of variation (C. V.) are reported in the subplot legends. Similar to Fig. 5, Fig. 6 suggests the BODi method is capable of conducting more diverse searches of the solution space (i.e., higher values of C.V.), which is likely due to the optimization of acquisition functions that lead the method to more fruitful parts of the space. Critically, such diverse search is the key to successfully locating performant left-turn restriction profiles.

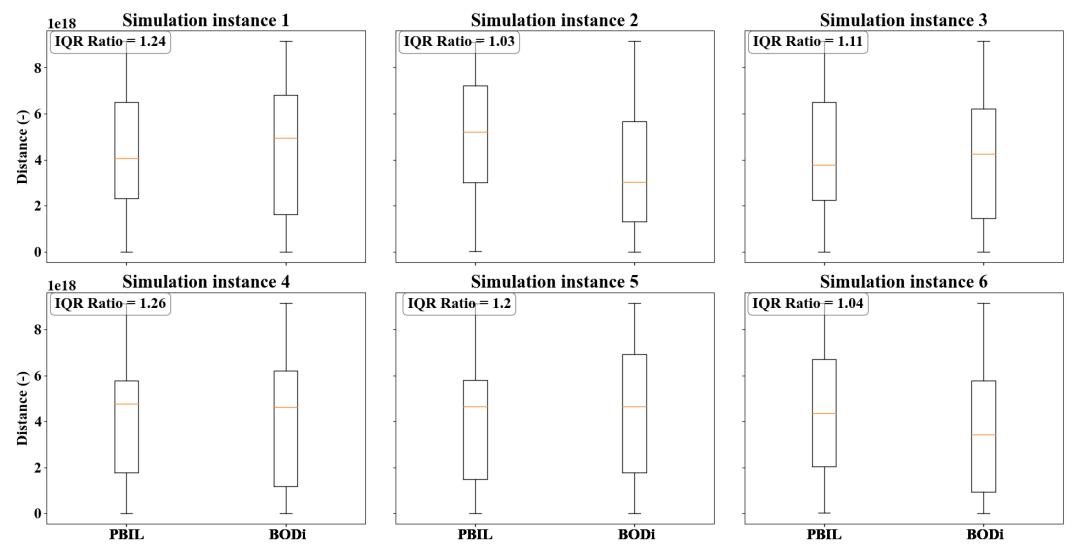


Fig. 5. Variability of solutions under each simulation instance.

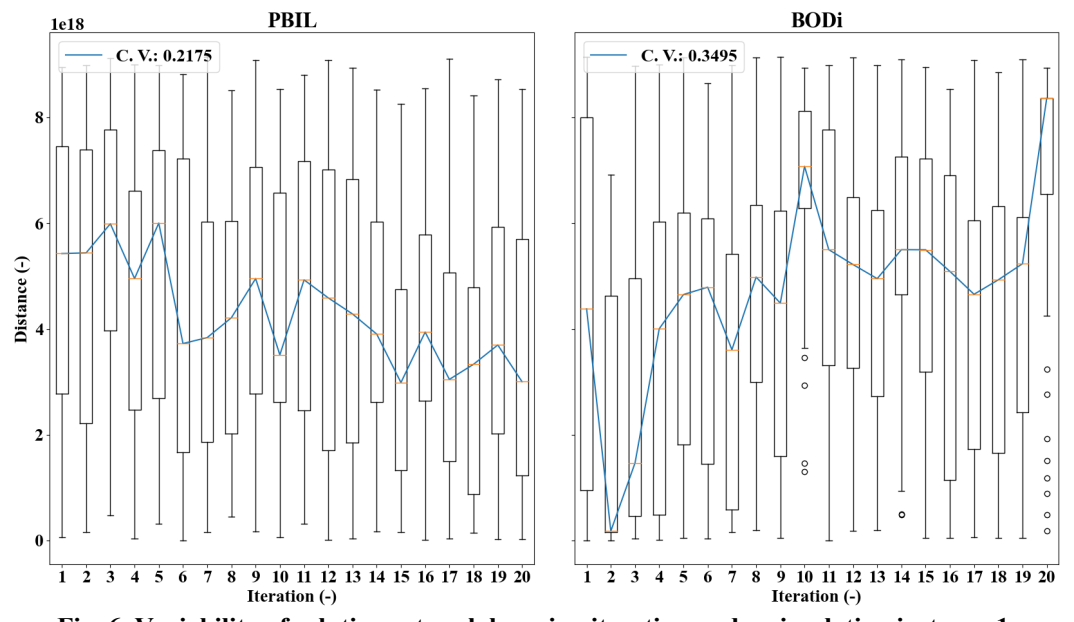


Fig. 6. Variability of solutions at each learning iteration under simulation instance 1.

The best-found configurations for each simulation instance using BODi are presented in Fig. 7, where a red dot indicates left-turn restriction. The PBIL configurations are omitted as it has been shown inferior to BODi. These configurations are also overlaid in Fig. 8, where the darker points represent locations with more common restriction decisions across the six simulation instances (the number of times restrictions are applied are also included for better readability). As can be seen, the left-turn restriction decisions are relatively more common in the central portion of the network (the central 4×4 area has a mean of 3.125 higher than the periphery of 2.409, with Welch's t-test p value being 0.031). This is reasonable as the central area has more routing options for drivers, thus restricting the left-turns here won't incur too much additional travel distance. On the other hand, the central area tends to serve the highest traffic flow, and the improved capacity from left-turn restriction (more lanes are dedicated to serving through-moving vehicles) helps save

travel time for the drivers. The travel time savings, coupled with a non-prominent addition of travel distances in the central area, leads to the overall reduced travel time for the whole network. The periphery locations, in comparison, do not have as many routes available and restricting left-turns will likely lead to significantly increased travel distances. Moreover, the periphery locations have lower traffic flows and the extra capacity from left-turn restrictions will likely be underutilized.

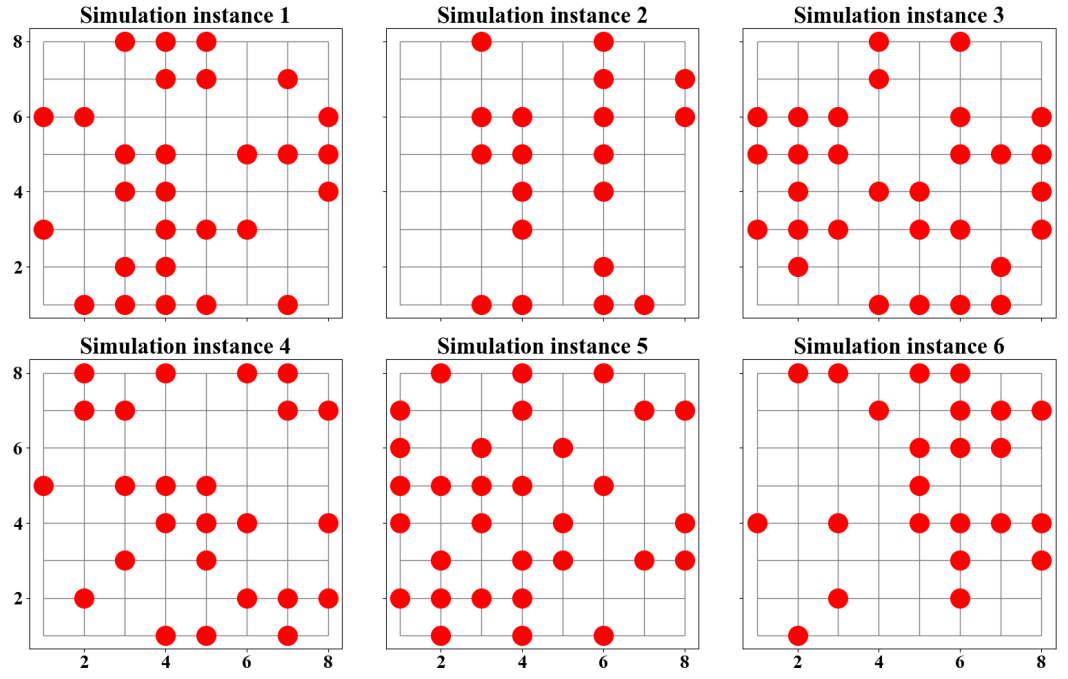


Fig. 7. The best left-turn restriction configurations for each simulation instance obtained by BODi.

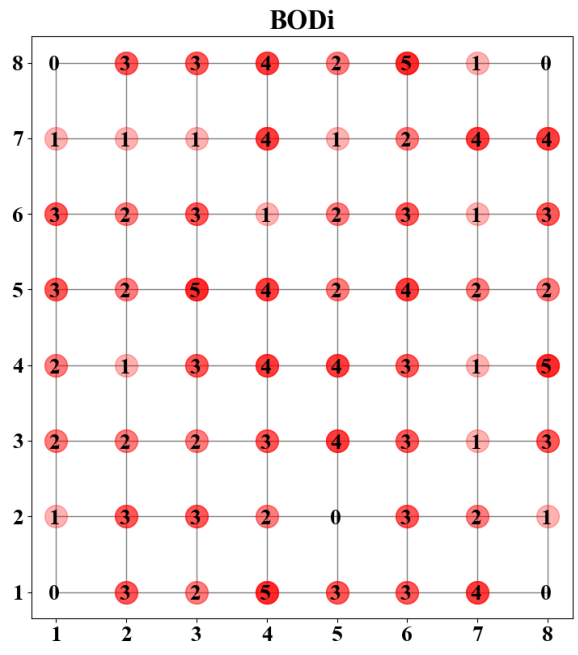


Fig. 8. The common restriction locations by BODi.

To examine the effectiveness of the BODi method in a more flexible left-turn restriction setting, the second optimization scenario (two decisions per intersection) is considered here. A single simulation instance (instance 1) is used for illustration purposes. The PBIL method, along with the baseline PLT and RLT configurations, is adopted for comparison, where the realized TTTs under the baseline configurations are the same as presented above. The dimensionality of the search space is considerably larger than the first scenario, and for this reason 10 optimization runs are conducted for both PBIL and BODi to report the best-found restriction configuration; see Fig. 9. Note, in this scenario each optimization run still evaluates at most 1000 left-turn restriction configurations and both methods adopt the same parameters as in the first scenario, hence it is more challenging for the methods to determine promising restriction profiles within the expanded solution space. As such, the best-found configurations by PBIL and BODi shown in Fig. 9 realize TTTs that are respectively 9.6% and 7.7% worse than reported in Fig. 4. However, in this scenario the restriction profile found by BODi saves 5.7% TTT compared to that found by PBIL, whereas the saving is 4.5% in the previous scenario where a single decision is made for each intersection. This suggests that the presented BODi method is more effective than PBIL at finding performant restriction configurations in higher-dimensional search spaces, as attributed to the dictionarybased embeddings that are suitable for handling high-dimensional structures.



545546

547548

549

550

551

527

528

529

530

531

532

533

534

535

536

537

538539

540

541542

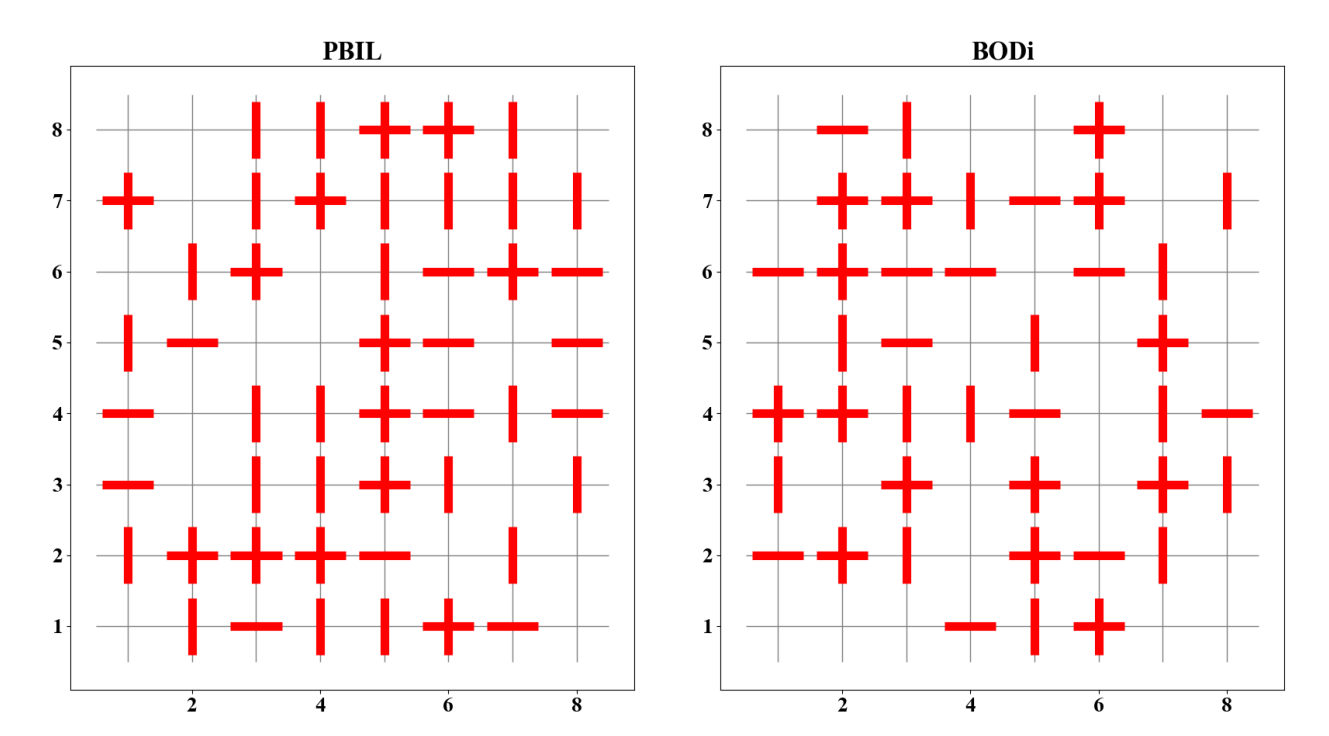


Fig. 9. The best left-turn restriction configurations for simulation instance 1 obtained by PBIL and BODi.

Overall, the results presented in this section show the BODi method can consistently find restriction configurations that yield smaller TTT than PBIL. Both methods can effectively utilize past experiences to arrive at better configurations that are consistent with engineering intuitions.

4.2 Imperfect Grid Network

To evaluate the generality of the proposed method, an imperfect grid network is considered herein. The imperfect network serves to both simulate more realistic traffic network structures and non-uniform traffic patterns since the network is no longer symmetric. A single random seed is used here which represents a certain trip generation sequence and OD pattern. Note the random seed is chosen at random so the results are generic. Both the PBIL and BODi are run three times and the best performing configuration is reported.

The evolutions of min TTT realized over iterations by PBIL and BODi are shown in Fig. 10, along with the TTTs under the baseline PLT and RLT configurations. The best-found restriction configurations are shown in Fig. 11. Note in particular that the TTT under RLT is significantly higher than in the perfect grid network (more than doubled). In part, this difference is due to the reduced number of routes between OD pairs, which thus requires more turning movements for the vehicles. As such, restricting all left turns leads to considerably more detours and thus more travel distances. The effect of the reduced number of routes can also be seen from the TTTs of both networks when all left turns are permitted. For this network, BODi and PBIL realize similar total travel times that are notably better than the baseline configurations, though BODi slightly outperforms the latter. The superior performances of these methods confirm their generality to more realistic settings.



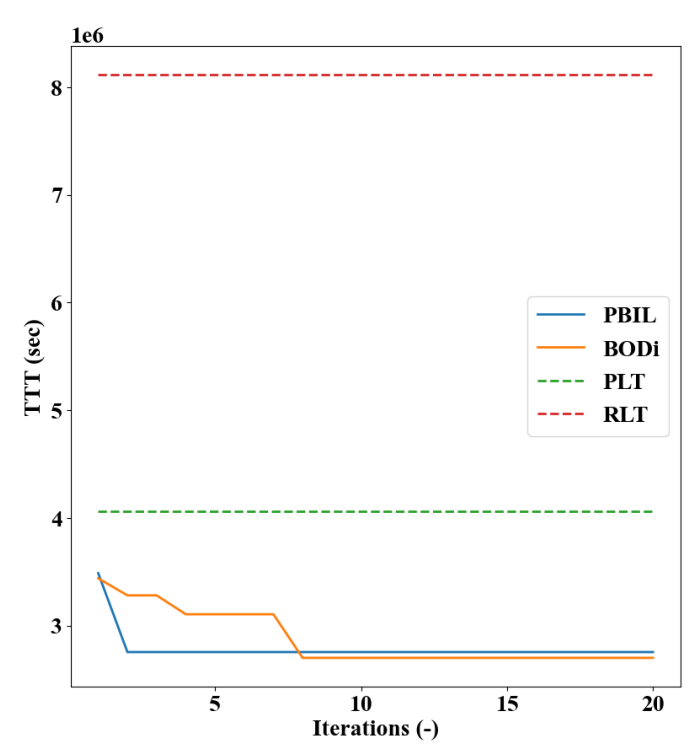


Fig. 10. Min TTT achieved over time by different methods for the imperfect network.

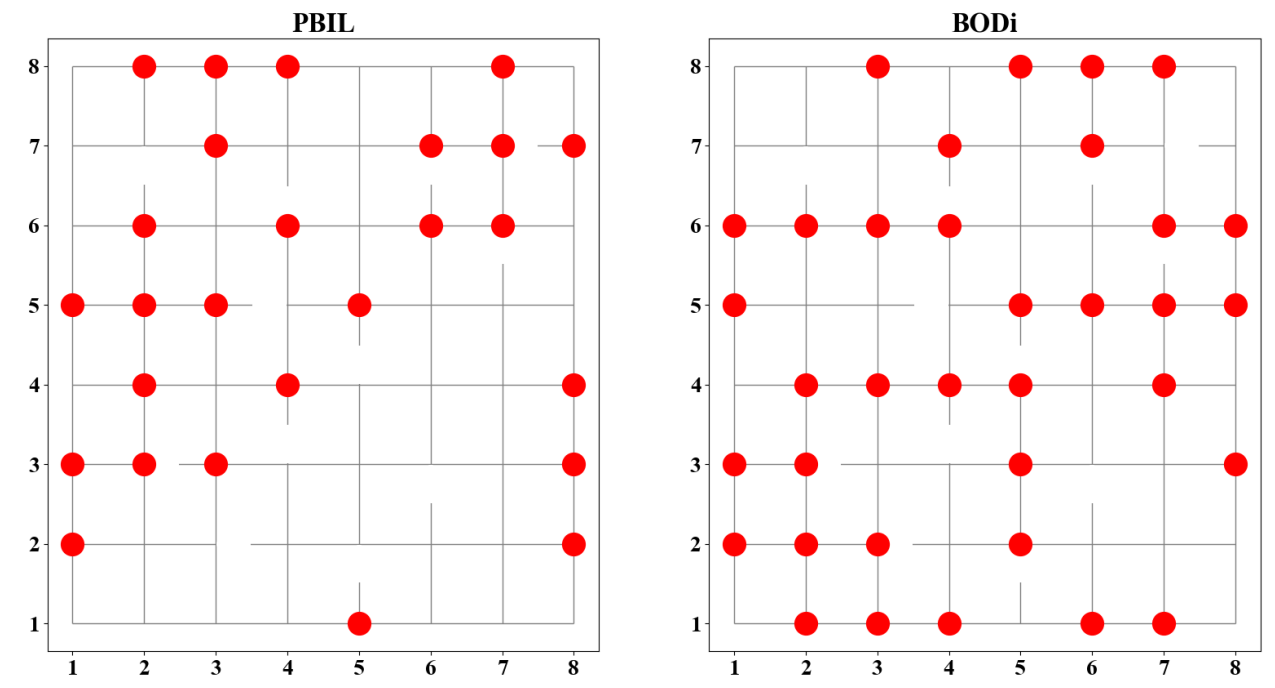


Fig. 11. The left-turn restriction profiles determined by PBIL and BODi for the imperfect network.

5. CONCLUDING REMARKS

This paper presents a novel Bayesian approach with a dictionary-based design to determining the optimal left-turn restriction locations in urban networks. This approach can effectively reduce the cardinality of the search space and accelerate the solution process. Simulation studies show the method can consistently find superior left-turn restriction profiles to PBIL and can often do so with less simulation cost. The solution quality with reduced simulation cost highlights the potential of the method on a range of traffic optimization problems, such as the optimal placement of bus lanes.

Future works should consider the joint optimization of left-turn restriction locations and signal timings. This problem still lies within the realm of black-box optimization but is much more challenging with combinatorial and continuous decision variables. Investigating the applicability of the presented method on more realistic traffic networks (for example by simulation of scenarios that consider protected left-turns and/or left-turn sight distance) should also be a research priority. Further, safety performance is implicitly considered here (by reducing conflicting maneuvers), and developing an explicit safety indicator is a promising direction. For practical implementation, one needs to account for the site-specific intersection configurations and demand patterns. The pipeline of network construction and simulation is transferable to field experiments, and the general trends of restricting left-turns at route-abundant areas with high traffic flows are likely to hold. An all-round assessment including environmental impacts such as emissions is also critical.

CREDIT AUTHORSHIP CONTRIBUTION STATEMENT

Dongqin Zhou: Conceptualization, Data curation, Formal analysis, Investigation, Methodology, Validation, Visualization, Writing – original draft, Writing – review & editing. Vikash V. Gayah: Conceptualization, Investigation, Supervision, Writing – review & editing.

DECLARATION OF COMPETING INTEREST

601 The authors declare that they have no known competing financial interests or personal 602

relationships that could have appeared to influence the work reported in this paper.

603 604

600

ACKNOWLEDGEMENTS AND DECLARATIONS

This research was supported by NSF Grant CMMI-1749200. The authors declare that the contents 605 of this article have not been published previously. All the authors have contributed to the work 606

607 described, read and approved the contents for publication in this journal.

608 609

REFERENCES

- 610 Baluja, S., 1994. Population-Based Incremental Learning. A Method for Integrating Genetic Search Based 611 Function Optimization and Competitive Learning. Pittsburgh, PA.
- 612 Baptista, R., Poloczek, M., 2018. Bayesian Optimization of Combinatorial Structures. 35th Int. Conf. Mach. 613 Learn. ICML 2018 2, 782-796.
- 614 Bayrak, M., Gayah, V. V., 2021. Identification of optimal left-turn restriction locations using heuristic 615 methods. Transp. Res. Rec. 2675, 452–467. https://doi.org/10.1177/03611981211011647
- 616 Bayrak, M., Yu, Z., Gayah, V. V., 2023. A population-based incremental learning algorithm to identify 617 optimal location of left-turn restrictions in urban grid networks. Transp. B Transp. Dyn. 11, 528–547. 618 https://doi.org/10.1080/21680566.2022.2102553
- 619 Berkowitz, C., Bragdon, C., Mier, F., 1996. Continuous flow intersection: A public private partnership. 620 VNIS 1996 - Veh. Navig. Inf. Syst. Conf. 277–287. https://doi.org/10.1109/VNIS.1996.1623758
- 621 Cascetta, E., Nuzzolo, A., Russo, F., Vitetta, A., 1996. A modified logit route choice model overcoming 622 path overlapping problems. Specification and some calibration results for interurban networks, in: 623 Proceedings of the 13th International Symposium on Transportation and Traffic Theory, Lyon, France, 624 pp. 697–711.
- 625 Chan, C.Y., 2006. Defining safety performance measures of driver-assistance systems for intersection left-626 turn conflicts. IEEE Intell. Veh. Symp. Proc. 25–30. https://doi.org/10.1109/IVS.2006.1689600
- 627 Chen, C., Wei, H., Xu, N., Zheng, G., Yang, M., Xiong, Y., Xu, K., Li, Z., 2020. Toward A Thousand 628 Lights: Decentralized Deep Reinforcement Learning for Large-Scale Traffic Signal Control. Proc. 629 AAAI Conf. Artif. Intell. 34, 3414–3421. https://doi.org/10.1609/aaai.v34i04.5744
- 630 Chowdhury, M.S., 2011. An Evaluation of New Jersey Jug-Handle Intersection (NJJI) with and without 631 Pre-Signals. T DI Congr. 2011 Integr. Transp. Dev. a Better Tomorrow - Proc. 1st Congr. Transp. 632 Dev. Inst. ASCE 1245–1254. https://doi.org/10.1061/41167(398)119
- 633 Chu, T., Wang, J., Codeca, L., Li, Z., 2020. Multi-agent deep reinforcement learning for large-scale traffic 634 Intell. 1086–1095. signal control. **IEEE** Trans. Transp. Syst. 21, 635 https://doi.org/10.1109/TITS.2019.2901791
- 636 Cottrell Jr, B.H., 1986. Guidelines for Protected/Permissive Left-Turn Signal Phasing. Transp. Res. Rec. J. 637 Transp. Res. Board 1069, 54–61.
- 638 Dadkhahi, H., Rios, J., Shanmugam, K., Das, P., 2022. Fourier Representations for Black-Box Optimization 639 over Categorical Variables. Proc. 36th AAAI Conf. Artif. Intell. AAAI 2022 36, 10156-10165. 640 https://doi.org/10.1609/aaai.v36i9.21255

- Dadkhahi, H., Shanmugam, K., Rios, J., Das, P., Hoffman, S.C., Loeffler, T.D., Sankaranarayanan, S., 2020.
- Combinatorial Black-Box Optimization with Expert Advice. Proc. ACM SIGKDD Int. Conf. Knowl.
- 643 Discov. Data Min. 1918–1927. https://doi.org/10.1145/3394486.3403243
- Daganzo, C.F., Gayah, V. V., Gonzales, E.J., 2011. Macroscopic relations of urban traffic variables:
- Bifurcations, multivaluedness and instability. Transp. Res. Part B Methodol. 45, 278–288.
- 646 https://doi.org/10.1016/j.trb.2010.06.006
- Daulton, S., Wan, X., Eriksson, D., Balandat, M., Osborne, M.A., Bakshy, E., 2022. Bayesian Optimization
- over Discrete and Mixed Spaces via Probabilistic Reparameterization. Adv. Neural Inf. Process. Syst.
- 649 35.
- DePrator, A.J., Hitchcock, O., Gayah, V. V, 2017. Improving urban street network efficiency by prohibiting conflicting left turns at signalized intersections. Transp. Res. Rec. 2622, 58–69.
- Deshwal, A., Ament, S., Balandat, M., Bakshy, E., Doppa, J.R., Eriksson, D., 2023. Bayesian Optimization
- over High-Dimensional Combinatorial Spaces via Dictionary-based Embeddings. Proc. Mach. Learn.
- 654 Res. 206, 7021–7039.
- 655 Eriksson, D., Jankowiak, M., 2021. High-Dimensional Bayesian Optimization with Sparse Axis-Aligned
- Subspaces. Proc. Mach. Learn. Res. 161, 493–503.
- 657 Eriksson, D., Pearce, M., Gardner, J.R., Turner, R., Poloczek, M., 2019. Scalable Global Optimization via
- Local Bayesian Optimization. Adv. Neural Inf. Process. Syst. 32.
- 659 Gayah, V., Daganzo, C., 2012. Analytical Capacity Comparison of One-Way and Two-Way Signalized Street Networks: Transp. Res. Rec. J. Transp. Res. Board 76–85. https://doi.org/10.3141/2301-09
- 661 Gayah, V. V., Daganzo, C.F., 2011. Clockwise hysteresis loops in the Macroscopic Fundamental Diagram:
- An effect of network instability. Transp. Res. Part B Methodol. 45, 643-655.
- https://doi.org/10.1016/j.trb.2010.11.006
- 664 Girault, J.T., Gayah, V. V., Guler, S.I., Menendez, M., 2016. Exploratory Analysis of Signal Coordination
- Impacts on Macroscopic Fundamental Diagram. https://doi.org/10.3141/2560-05 2560, 36-46.
- 666 https://doi.org/10.3141/2560-05
- Haddad, J., Geroliminis, N., 2013. Effect of Left Turns for Arterials with Queue Spillbacks, in:
- Transportation Research Board 92nd Annual Meeting. Washington D.C.
- Jones, D.R., Schonlau, M., Welch, W.J., 1998. Efficient Global Optimization of Expensive Black-Box
- Functions. J. Glob. Optim. 13, 455–492. https://doi.org/10.1023/A:1008306431147
- Joseph, H., John, R., 2000. Unconventional left-turn alternatives for urban and suburban arterials: an update.
- 672 Transp. Res. Circ. 17 p.-17 p.
- Messer, C.J., Fambro, D.B., 1977. Effects of Signal Phasing and Length of Left-Turn Bay on Capacity.
- Transp. Res. Rec. J. Transp. Res. Board 95–101.
- Newell, G.F., 1959. The effect of left turns on the capacity of a traffic intersection. Q. Appl. Math. 17, 67–
- 676 76. https://doi.org/10.1090/QAM/103121
- Oh, C., Tomczak, J.M., Gavves, E., Welling, M., 2019. Combinatorial Bayesian Optimization using the
- 678 Graph Cartesian Product. Adv. Neural Inf. Process. Syst. 32.
- Ortigosa, J., Gayah, V. V., Menendez, M., 2017. Analysis of one-way and two-way street configurations
- on urban grid networks. Transp. B Transp. Dyn. 7, 61-81.
- 681 https://doi.org/10.1080/21680566.2017.1337528
- Ortigosa, J., Menendez, M., Gayah, V. V., 2019. Analysis of Network Exit Functions for Various Urban

- 683 Grid Network Configurations. https://doi.org/10.3141/2491-02 2491, 12–21. https://doi.org/10.3141/2491-02
- Papenmeier, L., Nardi, L., Poloczek, M., 2023. Increasing the Scope as You Learn: Adaptive Bayesian Optimization in Nested Subspaces.
- Pelikan, M., Goldberg, D.E., Cantt U-Paz, E., n.d. BOA: The Bayesian Optimization Algorithm. https://doi.org/10.5555/2933923
- Rasmussen, C.E., Williams, C.K.I., 2006. Gaussian Processes for Machine Learning. The MIT Press.
- Reid, J.D., Hummer, J.E., 2001. Travel Time Comparisons Between Seven Unconventional Arterial Intersection Designs. https://doi.org/10.3141/1751-07 56-66. https://doi.org/10.3141/1751-07
- Roess, R.P., Prassas, E.S., McShane, W.R., 2010. Traffic Engineering 4th Ed. Pearson.
- Ru, B., Alvi, A.S., Nguyen, V., Osborne, M.A., Roberts, S.J., 2019. Bayesian Optimisation over Multiple Continuous and Categorical Inputs. 37th Int. Conf. Mach. Learn. ICML 2020 PartF168147-11, 8246– 8255.
- Snoek, J., Larochelle, H., Adams, R.P., 2012. Practical Bayesian Optimization of Machine Learning Algorithms. Adv. Neural Inf. Process. Syst. 4, 2951–2959.
- 698 Stemley, J., 1998. One-Way Streets Provide Superior Safety and Convenience. ITE J. 68, 47–50.
- Tang, Q., Friedrich, B., 2018. Design of signal timing plan for urban signalized networks including left turn prohibition. J. Adv. Transp. https://doi.org/10.1155/2018/1645475
- Tang, Q., Friedrich, B., 2016. Minimization of Travel Time in Signalized Networks by Prohibiting Left Turns. Transp. Res. Procedia 14, 3446–3455. https://doi.org/10.1016/J.TRPRO.2016.05.306
- 703 Turner, R., Eriksson, D., McCourt, M., Kiili, J., Laaksonen, E., Xu, Z., Guyon, I., 2021. Bayesian 704 Optimization is Superior to Random Search for Machine Learning Hyperparameter Tuning: Analysis 705 of the Black-Box Optimization Challenge 2020. Proc. Mach. Learn. Res. 133, 3–26.
- Walker, G.W., Kulash, W.M., McHugh, B.T., 2000. Downtown Streets: Are We Strangling Ourselves on One-Way Networks? Transp. Res. Circ.
- Wan, X., Nguyen, V., Ha, H., Ru, B., Lu, C., Osborne, M.A., 2021. Think Global and Act Local: Bayesian
 Optimisation over High-Dimensional Categorical and Mixed Search Spaces. Proc. Mach. Learn. Res.
 139, 10663–10674.
- Wazana, A., Rynard, V.L., Raina, P., Krueger, P., Chambers, L.W., 2000. Are Child Pedestrians at Increased Risk of Injury on One-way Compared to Two-way Streets? Can. J. Public Health 91, 201. https://doi.org/10.1007/BF03404272
- Wei, H., Xu, N., Zhang, H., Zheng, G., Zang, X., Chen, C., Zhang, W., Zhu, Y., Xu, K., Li, Z., 2019.
 CoLight: Learning Network-level Cooperation for Traffic Signal Control 1913–1922.
 https://doi.org/10.1145/3357384.3357902
- Wei, H., Zheng, G., Yao, H., Li, Z., 2018. Intellilight: A reinforcement learning approach for intelligent traffic light control, in: Proceedings of the 24th ACM SIGKDD International Conference on Knowledge Discovery & Data Mining. pp. 2496–2505.
- 720 Xuan, Y., Daganzo, C.F., Cassidy, M.J., 2011. Increasing the capacity of signalized intersections with 721 separate left turn phases. Transp. Res. Part В Methodol. 45, 769–781. 722 https://doi.org/10.1016/J.TRB.2011.02.009